

Supplementary Information

The Giant Electrorheological Fluid with Long Lifetime and Good Thermal Stability Based on TiO₂ Inlaid with Nanocarbons

Zhaohui Qiu¹, Rong Shen², Jing Huang¹, Kunquan Lu², Xiaomin Xiong^{1*}

¹ School of Physics, Sun Yat-sen University, Guangzhou 510275, China

² Beijing National Laboratory for Condensed Matter Physics, Key Laboratory of Soft Matter Physics, Institute of Physics,
Chinese Academy of Sciences, Beijing 100190, China

1. Estimate

As shown in Figure 1(c) and (e), two TiO₂ spheres with a dielectric constant of ϵ_p , radius of R and gap of D were placed in a uniform external electric field. The dielectric constant of the surrounding medium was ϵ_f , and when $\epsilon_p/\epsilon_f \approx 100$, and $D \approx 10^{-3}R$, the intensity of the local field (E_{loc}) in the gap was 10^3 times larger than that of the external field (E_0)^[1]. There are nanocarbon clusters with a radius of r in the gap. Carbon is a semi-metal, and nanocarbon clusters were treated as spherical conductors. In the gap between TiO₂ particles, because $D \ll R$, the surfaces could be treated as parallel plates. The dipole moment approximation was applied for the derivations below.

According to the Gauss theorem, the polar charge surface density could be expressed as,

$$\sigma = \frac{(\epsilon_p - \epsilon_f)}{2\epsilon_p} \epsilon_0 E_{loc} \approx \frac{\epsilon_0 E_{loc}}{2} \quad (1)$$

On the surface of the dielectric particles, next to the carbon clusters, the quantity of the polar charge on the surface of the dielectric particle along the direction of the external electric field could be expressed as

$$Q = \sigma s = \frac{\epsilon_0 E_{loc} s}{2} \quad (2)$$

where $s = \pi r^2$ and is the area of a circle with a radius of r .

According to Coulomb's law, the interaction forces among polar charges could be expressed as,

$$F_{Q-Q} = \frac{Q^2}{4\pi\epsilon_f\epsilon_0 D^2} = \frac{\epsilon_0 E_{loc}^2 s^2}{16\pi\epsilon_f D^2} \quad (3)$$

The induced dipole moment of a carbon cluster in a local field could be expressed as^[2],

$$\mu = 4\pi\epsilon_f\epsilon_0 r^3 E_{loc} \quad (4)$$

* Email: xiongxm@mail.sysu.edu.cn

When $r=1$ nm, from equation (4), the induced dipole moment of carbon cluster $\mu=83$ Debye.

The interaction forces between the induced dipole moment of a spherical conductor and polar charges on the surfaces of adjacent TiO_2 particles was expressed as,

$$F_{Q-C} = \frac{Q\mu/2r}{4\pi\epsilon_r\epsilon_0} \left(\frac{1}{d^2} - \frac{1}{(d+2r)^2} \right) = \frac{\epsilon_0 E_{\text{loc}}^2 s r^3 (r+d)}{d^2 (2r+d)^2} \quad (5)$$

where d is the distance between carbon clusters and polar charges on the TiO_2 particles. When $r=1$ nm, $D=d$, $d=0.1r$, and the ratio of F_{Q-Q} and F_{Q-C} is about up to 10.

The interaction forces between two induced dipole moments of spherical conductors is expressed as,

$$F_{C-C} = \frac{(\mu/2r)^2}{4\pi\epsilon_f\epsilon_0} \left(\frac{1}{\delta^2} - \frac{2}{(2r+\delta)^2} + \frac{1}{(4r+\delta)^2} \right) \quad (6)$$

where δ is the distance between two carbon clusters, and if $r=1$ nm, $D=\delta=0.1r$, and the ratio of F_{Q-Q} and F_{C-C} is about 100.

The area in between the particles separated by $D=2r$ is nearly $s=\pi R D/2$, where interactions occur effectively. In this region the number of F_{Q-Q} is $n_1=s/\pi r^2$, and the the number of F_{Q-C} and F_{C-C} (n_2, n_3) depend on the number density of nanocarbon. The interaction forces between two adjacent particles is expressed as,

$$F_{P-P} = n_1 F_{Q-Q} + n_2 F_{Q-C} + n_3 F_{C-C} \quad (7)$$

Where n_1, n_2, n_3 is the number of interaction forces in a unit area.

The number of the particle chains in a unit area is $N=3\varphi/(2\pi R^2)$, where φ is the volume fraction of the particles in the suspension. Thus, the shear stress can be approximately expressed as [3]

$$\tau \approx N * F_{P-P} \quad (8)$$

As an example, we consider a system of $R=1\mu\text{m}$, $\varphi=33\%$, $r=1\text{nm}$, $n_1=2n_2=4n_3$, $E=3\text{kV/mm}$. The shear stress equal approximately to 37kPa.

In addition, the relationship between the shear stress and the size of particles was calculated. The ratio of the local field E_{loc} to the applied field E_0 was obtained as $E_{\text{loc}}/E_0=(2R+D)/D \approx 2R/D$ [4]. From the equation (3), (5), (6), (7), the interaction force between two adjacent particles F_{P-P} is proportional to E_{loc}^2 (i.e. R^2). On the other hands the number of the particle chains in a unit area N is proportional to R^{-2} . Therefore, the shear stress of the novel ER fluid ($\tau=N*F_{P-P}$) dose not change with the R .

2. XRD

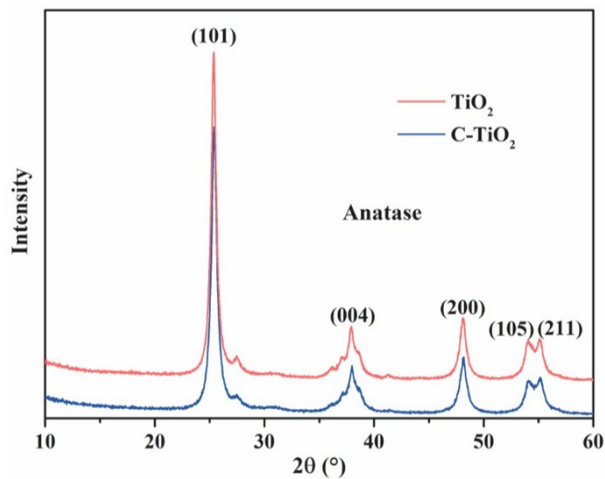


Figure S1 XRD pattern of TiO₂ and C+TiO₂ particles

The powder X-ray diffraction (XRD) measurement was performed on a Rigaku D-MAX 2200 X-ray diffractometer with CuKα irradiation. Figure S1 shows that both the TiO₂ and C-TiO₂ particles are the anatase.

3. Particle size and distribution

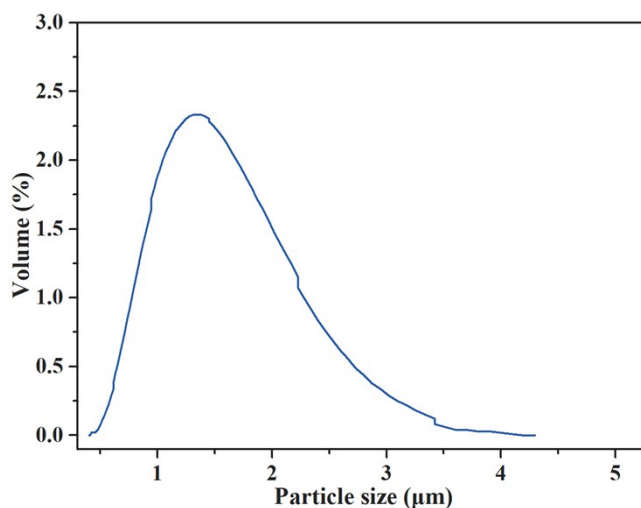


Figure S2 Particle size and distribution of C-TiO₂ particles (d(0.1)=0.836μm, d(0.5)=1.431μm, d(0.9)=2.444μm)

The Particle size and distribution of C-TiO₂ were acquired by Malvern MasterSizer 2000.

4. TEM

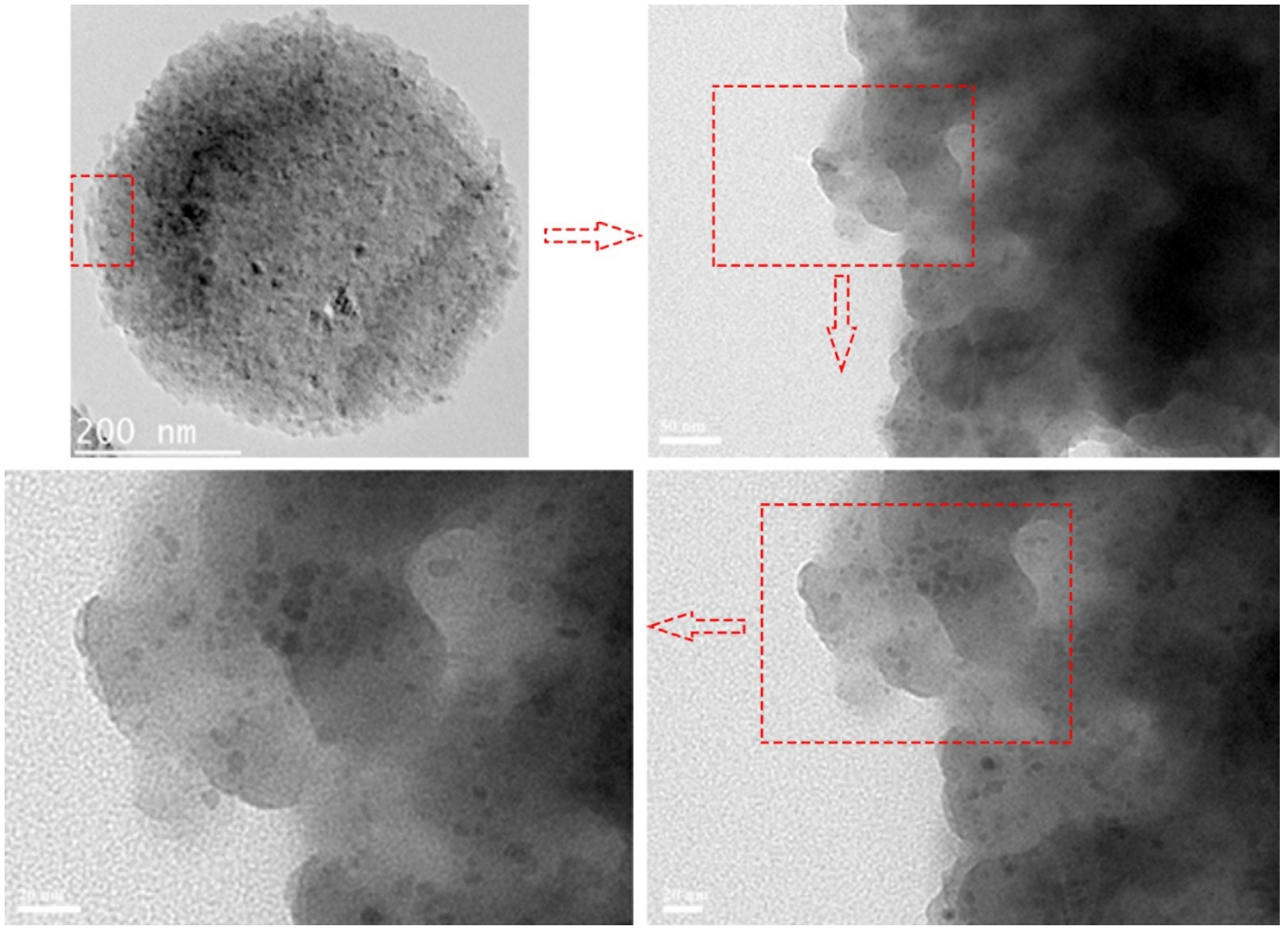


Figure S3 TEM images of the edge of one C-TiO₂ particle. The black dots in the TiO₂ particles are nanocarbon clusters.

5. Dielectric spectra

The dielectric constant of the TiO₂ nano-particles is much higher than that of the bulk materials^[5,6]. The dielectric constant of the C-TiO₂ particles ϵ_p was measured by Agilent 4284A using powder pressed method, and $\epsilon_p=212$.

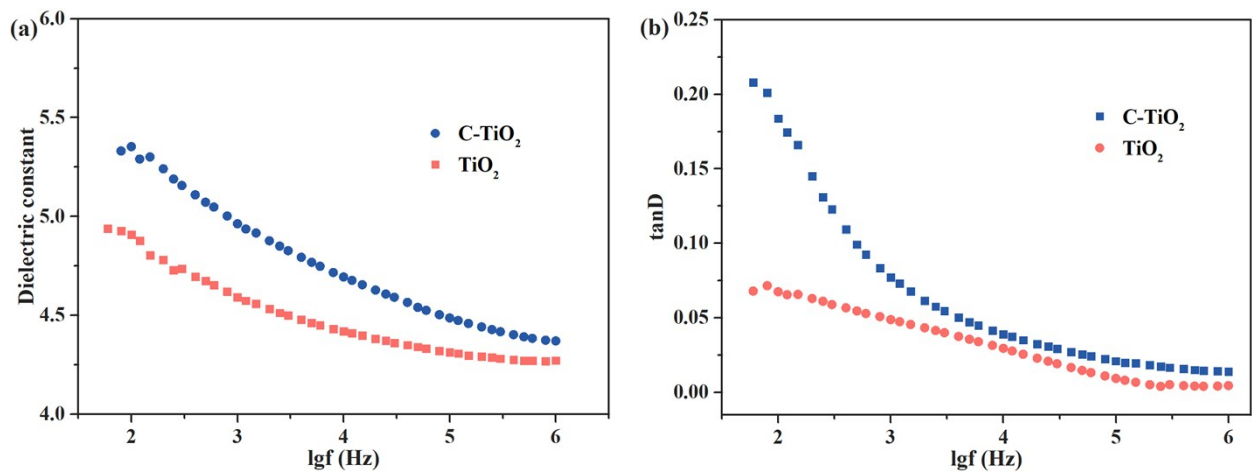


Figure S4 (a) Dielectric constants of the ER fluid (TiO₂ and C-TiO₂, $\phi=33\%$) plotted as a function of frequency.

(b) Dielectric loss tangents of the ER fluid (TiO_2 and C- TiO_2 , $\phi=33\%$) plotted as a function of frequency.

The dielectric spectra of the ER fluids were acquired by Agilent 4284A. As Figure S4 shown, dielectric constant and dielectric loss of C- TiO_2 -ER fluid are larger than that of the TiO_2 , especially at the low frequency region. The higher dielectric constant of particles causes the higher local electric field at the gap of adjacent TiO_2 . The high dielectric loss produce a large amount of thermal energy which that can easily drive particles to move and form chains^[7]. It also explains that the shear stress of C- TiO_2 -ER fluid is higher than that of the TiO_2 .

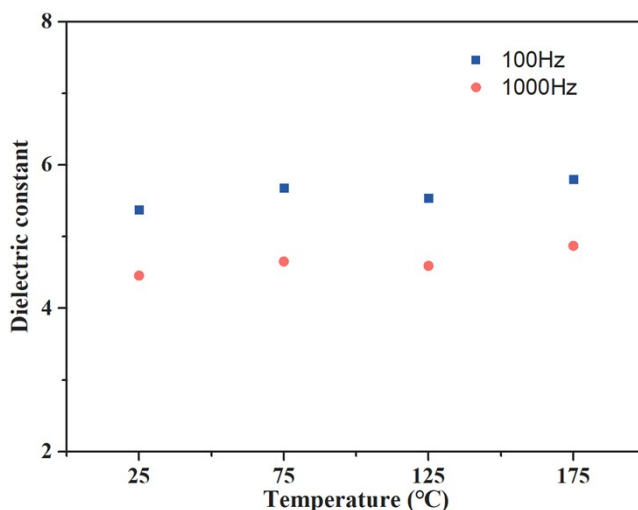


Figure S5 Dielectric constant of the C- TiO_2 -ER fluid ($\phi=33\%$) plotted as a function of temperatures for two testing frequency.

6. Characterization of ER fluids

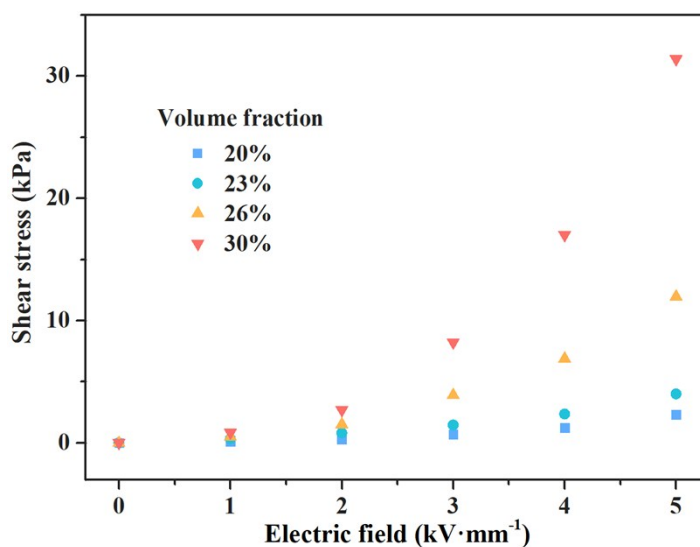


Figure S6 Shear stress of the ER fluid ($\phi=20, 23, 26, 30\%$) plotted as a function of the electric field intensity

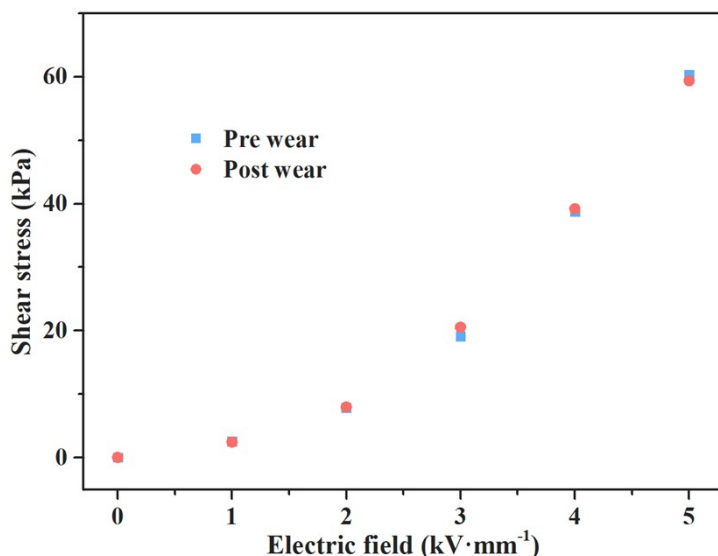


Figure S7 Shear stress of the ER fluid plotted as a function of the electric field intensity for pre-/post-wear ($\phi=33\%$) conditions (without applying electric field, 500 hours)

7. Effect of nanocarbon on ER fluids

We tried to control the size of nanocarbon by changing the amount of glucose and the size of nanocarbon increases with increasing of the amount of glucose (Figure S8). Figure S9 shows that the shear stress is first increased and then decreased along with the increasing of the amount of the glucose. When the amount of glucose is low (<1g), the size of nanocarbon particles is small, but the number density is also small, so the shear stress is low in this case. When the amount of glucose is greater than 1g, the size of carbon particles increases obviously and the number density is also large, but the shear stress decreases. Therefore, we can surmise that, when the number density is constant, the smaller the nanocarbon is, the easier it is to exist in the small gap between TiO₂ particles, i.e. in the local electric field, the greater the shear stress is.

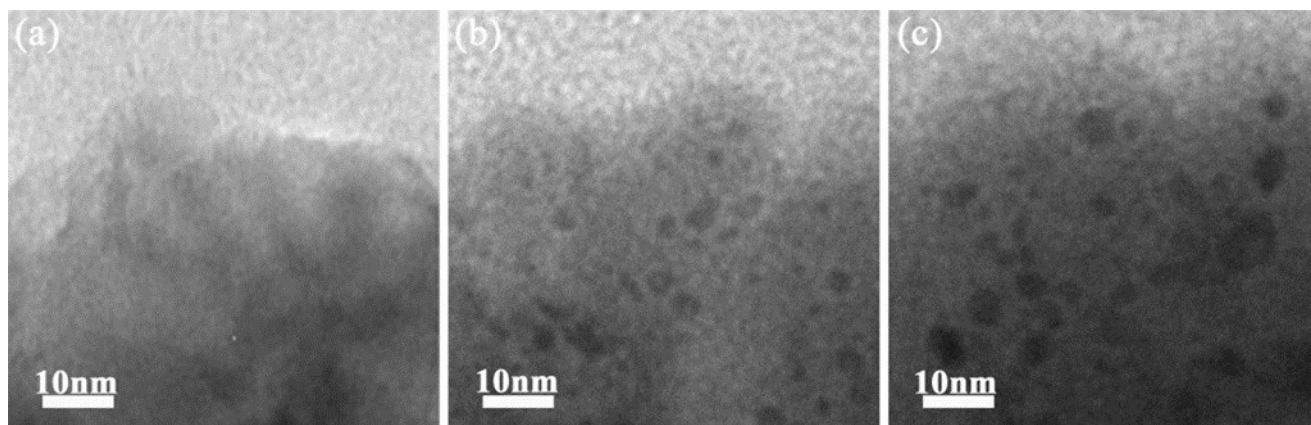


Figure S8 TEM images of the edge of C-TiO₂ particle with different amounts of glucose (a) 0g, (b) 0.5, (c) 2g.

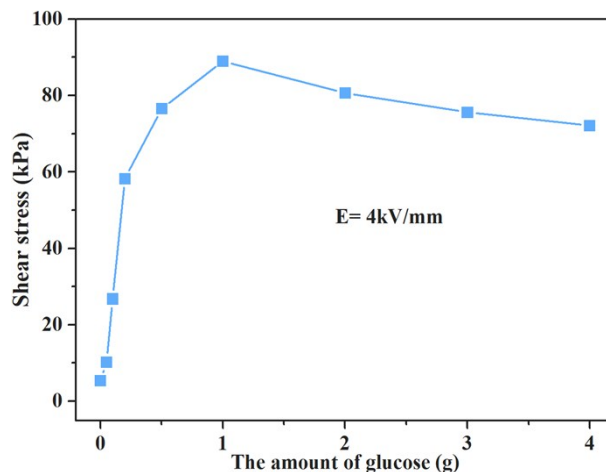


Figure S9 Shear stress of the ER fluids consisted of different C-TiO₂ powder with different amounts of glucose plotted as a function of the amount of glucose

The prepared C-TiO₂ powders were treated at 300°C in air with different time to reduce the nanocarbon content gradually. As can be seen from Figure S10, the powders gradually change from black to grey as the processing time to extend, which indicates that the nanocarbon is oxidized and the number density decreases. These powders were mixed with oil and the ER fluids ($\phi=38\%$) were obtain. As shown in Figure S11, the shear stress of the ER fluids consisted of C-TiO₂ particles with different treatment time decrease with the increase of the treatment time, which illustrates that ER effect depends on the number density of carbon.

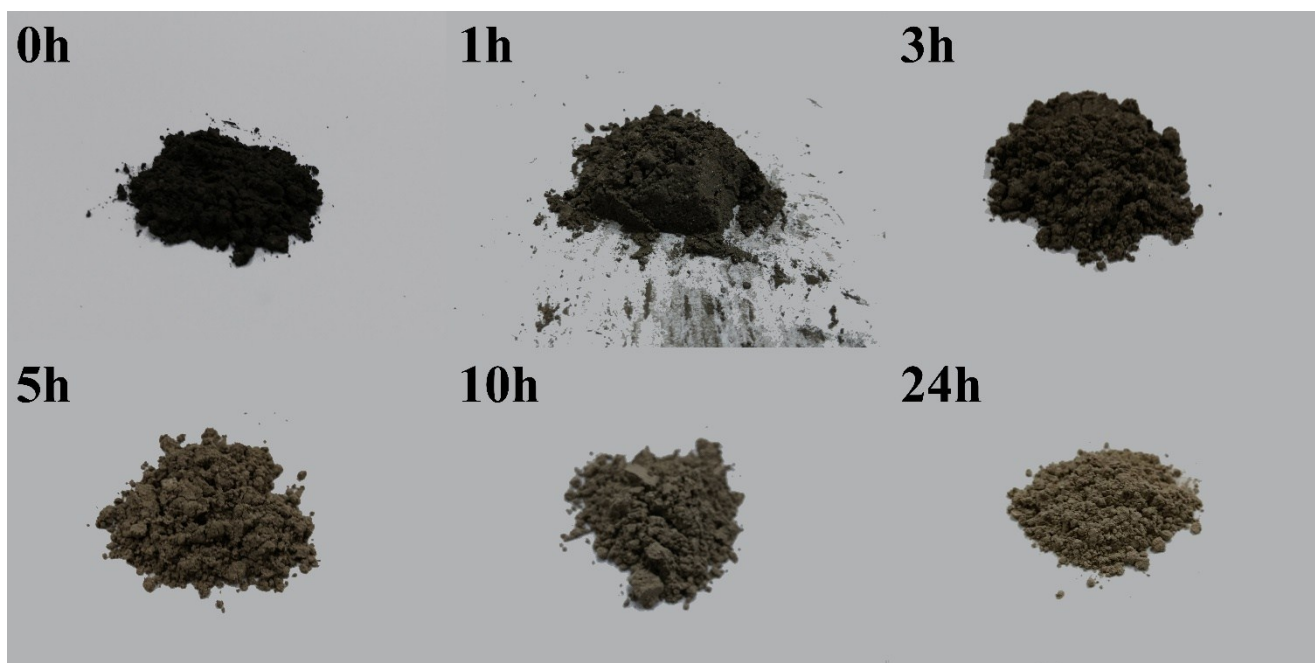


Figure S10 Photos of the different C-TiO₂ powder with different treatment time.

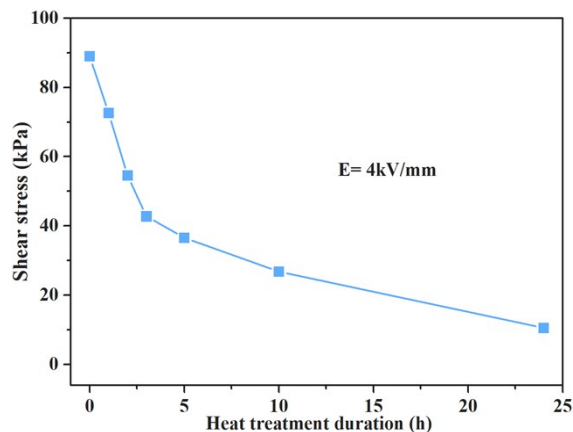


Figure S11 Shear stress of the ER fluids consisted of different C-TiO₂ powder with different treatment time plotted as a function of the heat treatment duration

8. The anti-settlement behavior of ER fluid

C-TiO₂ particles are wetted well by oil with the wetting angle of 30° and oil has a high viscosity (300cSt), so C-TiO₂-ER fluid did not settle down apparently (<1%) after half year, showing a good anti-sedimentation property.

References

1. L. C. Davis, *J. Appl. Phys.*, 1997, **81**, 1985-1991.
2. K. Q. Lu, J. X. Liu, *Introduction to soft matter physics*; Peking University Press Beijing: Beijing, China, 2006.
3. K. Lu, R. Shen, Z. Wang, S. Gang, W. Wen and J. Liu, *Chinese. Phys.*, 2006, **15**, 2476-2480.
4. H. Jie, M. Shen, J. Xu, W. X. Chen, Y. Jin, W. N. Peng, X. B. Fu and L. W. Zhou, *Appl. Phys. Lett.*, 2004, **85**, 2646-2648.
5. T. Hao, *Appl. Phys. Lett.*, 1997, **70**, 1956-1958.
6. L. D. Zhang, H. F. Zhang, G. Z. Wang, C. M. Mo and Y. Zhang, *Phys. Status solidi A*, 1996, **157**, 483-491.
7. A. Dey, S. De, A. De and S. K. De, *Nanotechnology*, 2004, **15**, 1277-1283.